

Addition of carbonic anhydrase 9 inhibitor SLC-0111 to temozolomide treatment delays glioblastoma growth in vivo

Nathaniel H. Boyd, ... , Shoukat Dedhar, Anita B. Hjelmeland

JCI Insight. 2017;2(24):e92928. <https://doi.org/10.1172/jci.insight.92928>.

Research Article

Neuroscience

Oncology

Tumor microenvironments can promote stem cell maintenance, tumor growth, and therapeutic resistance, findings linked by the tumor-initiating cell hypothesis. Standard of care for glioblastoma (GBM) includes temozolomide chemotherapy, which is not curative, due, in part, to residual therapy-resistant brain tumor-initiating cells (BTICs). Temozolomide efficacy may be increased by targeting carbonic anhydrase 9 (CA9), a hypoxia-responsive gene important for maintaining the altered pH gradient of tumor cells. Using patient-derived GBM xenograft cells, we explored whether CA9 and CA12 inhibitor SLC-0111 could decrease GBM growth in combination with temozolomide or influence percentages of BTICs after chemotherapy. In multiple GBMs, SLC-0111 used concurrently with temozolomide reduced cell growth and induced cell cycle arrest via DNA damage in vitro. In addition, this treatment shifted tumor metabolism to a suppressed bioenergetic state in vivo. SLC-0111 also inhibited the enrichment of BTICs after temozolomide treatment determined via CD133 expression and neurosphere formation capacity. GBM xenografts treated with SLC-0111 in combination with temozolomide regressed significantly, and this effect was greater than that of temozolomide or SLC-0111 alone. We determined that SLC-0111 improves the efficacy of temozolomide to extend survival of GBM-bearing mice and should be explored as a treatment strategy in combination with current standard of care.

Find the latest version:

<https://jci.me/92928/pdf>



Addition of carbonic anhydrase 9 inhibitor SLC-0111 to temozolomide treatment delays glioblastoma growth in vivo

Nathaniel H. Boyd,¹ Kiera Walker,¹ Joshua Fried,² James R. Hackney,³ Paul C. McDonald,⁴ Gloria A. Benavides,^{3,5} Raffaella Spina,⁶ Alessandra Audia,⁷ Sarah E. Scott,¹ Catherine J. Landis,¹ Anh Nhat Tran,¹ Mark O. Bevenssee,¹ Corinne Griguer,⁸ Susan Nozell,⁹ G. Yancey Gillespie,⁸ Burt Nabors,¹⁰ Krishna P. Bhat,⁷ Eli E. Bar,⁶ Victor Darley-Usmar,^{3,5} Bo Xu,² Emily Gordon,¹¹ Sara J. Cooper,¹¹ Shoukat Dedhar,⁴ and Anita B. Hjelmeland¹

¹Department of Cell, Developmental and Integrative Biology, University of Alabama at Birmingham, Birmingham, Alabama, USA. ²Department of Oncology, Southern Research Institute, Birmingham, Alabama, USA. ³Department of Pathology, University of Alabama at Birmingham, Birmingham, Alabama, USA. ⁴Department of Integrative Oncology, BC Cancer Research Centre, Vancouver, British Columbia, Canada. ⁵Center for Free Radical Biology, University of Alabama at Birmingham, Birmingham, Alabama, USA. ⁶Department of Neurological Surgery, Case Western University, Cleveland, Ohio, USA. ⁷Department of Translational Molecular Pathology, MD Anderson Cancer Center, Houston, Texas, USA. ⁸Department of Neurosurgery, ⁹Department of Radiation Oncology, and ¹⁰Department of Neurology, University of Alabama at Birmingham, Birmingham, Alabama, USA. ¹¹HudsonAlpha Institute for Biotechnology, Huntsville, Alabama, USA.

Tumor microenvironments can promote stem cell maintenance, tumor growth, and therapeutic resistance, findings linked by the tumor-initiating cell hypothesis. Standard of care for glioblastoma (GBM) includes temozolomide chemotherapy, which is not curative, due, in part, to residual therapy-resistant brain tumor-initiating cells (BTICs). Temozolomide efficacy may be increased by targeting carbonic anhydrase 9 (CA9), a hypoxia-responsive gene important for maintaining the altered pH gradient of tumor cells. Using patient-derived GBM xenograft cells, we explored whether CA9 and CA12 inhibitor SLC-0111 could decrease GBM growth in combination with temozolomide or influence percentages of BTICs after chemotherapy. In multiple GBMs, SLC-0111 used concurrently with temozolomide reduced cell growth and induced cell cycle arrest via DNA damage in vitro. In addition, this treatment shifted tumor metabolism to a suppressed bioenergetic state in vivo. SLC-0111 also inhibited the enrichment of BTICs after temozolomide treatment determined via CD133 expression and neurosphere formation capacity. GBM xenografts treated with SLC-0111 in combination with temozolomide regressed significantly, and this effect was greater than that of temozolomide or SLC-0111 alone. We determined that SLC-0111 improves the efficacy of temozolomide to extend survival of GBM-bearing mice and should be explored as a treatment strategy in combination with current standard of care.

Authorship note: N.H. Boyd and K. Walker contributed equally to this work.

Conflict of interest: S. Dedhar and P.C. McDonald are inventors of SLC-0111, which is under development by Wellichem Biotech Inc. Wellichem Biotech Inc. provided the vehicle and oral formulation of SLC-0111 for in vivo trials but no other financial support.

Submitted: January 20, 2017

Accepted: October 23, 2017

Published: December 7, 2017

Reference information:

JCI Insight. 2017;2(23):e92928.

<https://doi.org/10.1172/jci.insight.92928>.

insight.92928.

Introduction

Glioblastoma (GBM), grade IV astrocytoma, is the most commonly diagnosed form of primary brain tumors in adults, and prognosis for these patients is extremely poor. Median time to recurrence is 6.9 months after treatment, which includes surgical resection, chemotherapy with the DNA-alkylating agent temozolomide (TMZ), and radiotherapy. Median overall survival is approximately 12–14 months (1–3), indicating an urgent need for novel therapeutic approaches. Development of these new approaches will be challenging, as GBM is extremely heterogeneous, with genetic, epigenetic, differentiation state, and micro-environmental differences. One subpopulation, called brain tumor-initiating cells (BTICs), is characterized by self-renewal properties, proliferation and differentiation potential, and neurosphere formation capability (4–6). Evidence suggests that BTICs are resistant to adjuvant therapies and thus contribute to tumor recurrence in GBM. Thus, research efforts have focused on understanding and targeting the BTIC population.

BTIC maintenance, GBM growth, and therapeutic response are all influenced by tumor microenvironments, with hypoxia being one of the most common and well-studied microenvironmental features of solid

tumors (7). Hypoxia occurs when tumors are unable to meet the need for increased vasculature to support the oxygen and nutrient supply of a growing tumor (8, 9). Hypoxia leads to a metabolic shift to glycolysis, which is facilitated by the metabolic plasticity of cancer cells (10). The shift to glycolysis results in an altered pH gradient with acidic extracellular space and an alkaline environment within the tumor cell (11, 12). In addition to modulating metabolism, hypoxia regulates cell growth, differentiation state, angiogenesis, and invasion (13, 14). These protumorigenic effects may also be similarly regulated by pH changes in the absence of hypoxia, proving the importance of targeting the tumor microenvironment to improve GBM patient therapies.

One hypoxia and acidic stress-induced target gene that is often used as a hypoxia marker is carbonic anhydrase 9 (*CA9*) (9, 15–20). Carbonic anhydrases are a family of metalloenzymes that catalyze the reversible conversion of carbon dioxide to bicarbonate and protons (20, 21). Relative to other family members, *CA9* is normally restricted to the gastrointestinal tract but is overexpressed in solid tumors, including GBM (22, 23). Thus, *CA9* inhibitors are expected to have reduced off-target effects relative to more broad carbonic anhydrase inhibitors. *CA9* is expressed on the plasma membrane of hypoxic tumor cells where it facilitates maintenance of an altered pH balance (external pH < internal pH) and adaptation to the altered tumor metabolism (20, 24, 25). *CA9* elevation in GBM and other cancers was also correlated with poor prognosis (18), although correlation with survival independent of other markers of hypoxia is not always clear. Genetic targeting of *CA9* with shRNA provided evidence of delayed tumor growth in breast and colon cancers as well as in the GBM cell line U87MG (18, 26, 27). Furthermore, sorting of breast cancer cells for *CA9* high populations enriched for breast cancer TIC markers and mammosphere formation provided a direct link between *CA9* and TIC phenotypes (28). In GBM, a prior report demonstrated that TMZ-induced apoptosis could be augmented in vitro when cells were pretreated with acetazolamide, a broad carbonic anhydrase inhibitor and diuretic (29, 30). However, the capacity of pharmacologic carbonic anhydrase inhibition to affect GBM growth in vivo remained unclear. SLC-0111 is a novel ureido-substituted benzenesulfonamide developed as a carbonic anhydrase inhibitor that is greater than 100 times more selective for tumor-associated *CA9* and *CA12* in comparison to the off-target, intracellular *CA1* and *CA2* (31). While other carbonic anhydrase inhibitors (acetazolamide, methazolamide, topiramate) are used clinically for the treatment of glaucoma, altitude sickness, and/or seizures, these drugs do not possess the favorable specificity for *CA9* exhibited by SLC-0111 (21). As SLC-0111 demonstrated efficacy against breast cancer xenografts (24, 27) and was in phase I clinical trials (NCT02215850), we sought to determine the potential of SLC-0111 for GBM patients. We investigated the hypothesis that SLC-0111 could decrease BTIC survival and chemoresistance to reduce GBM growth in vivo.

Results

Carbonic anhydrase gene family expression in astrocytes and GBM patient-derived xenograft cells. To evaluate the potential utility of a *CA9*- and *CA12*-specific inhibitor against GBM, we first determined the expression of carbonic anhydrase family members in cells isolated from a pediatric primary (D456) and a recurrent (1016) GBM patient-derived xenograft (PDX) as well as immortalized but nontumorigenic human astrocytes (Figure 1). We evaluated levels of *CA2*, *CA4*, *CA6*, *CA9*, *CA12*, and *CA13*, as these family members had been previously implicated as being important for tumor biology and/or pH regulation. When GBM PDX cells cultured in normoxia (21% O₂) and hypoxia (2% O₂) were compared, we observed minimal changes in *CA2* and *CA6* and variable changes in *CA4*, *CA12*, and *CA13* (Figure 1A and data not shown). In contrast, *CA9* was upregulated by hypoxia more than 100-fold in all GBM PDX cells evaluated, consistent with *CA9* as a known hypoxia-induced gene in solid tumors (Figure 1, A and B, and data not shown). We also observed *CA12* induction in both GBM and astrocytes in hypoxia (Figure 1A), suggesting that *CA12* is also hypoxia regulated in the brain. Higher levels of *CA2*, *CA4*, *CA6*, or *CA13* did not trend with worse patient prognosis in GBM when evaluated using The Cancer Genome Atlas data accessed via GlioVis (ref. 32 and Supplemental Figure 1; supplemental material available online with this article; <https://doi.org/10.1172/jci.insight.92928DS1>) (33, 34). In contrast, elevated *CA9* and *CA12* expression both correlated or trended with poor GBM patient outcomes (Figure 1C), particularly in the proneural subtype (Supplemental Figure 2). More significant associations between higher *CA9* and *CA12* expression and reduced patient survival were observed in data from both high- and low-grade gliomas (Figure 1D), likely due to the increased levels of *CA9* and *CA12* mRNA in GBM relative to lower grade gliomas (Figure 1E). These data are consistent with prior immunohistochemical data, demonstrating that elevated *CA9* does suggest a higher chance for poor survival (23). Together, the data confirmed

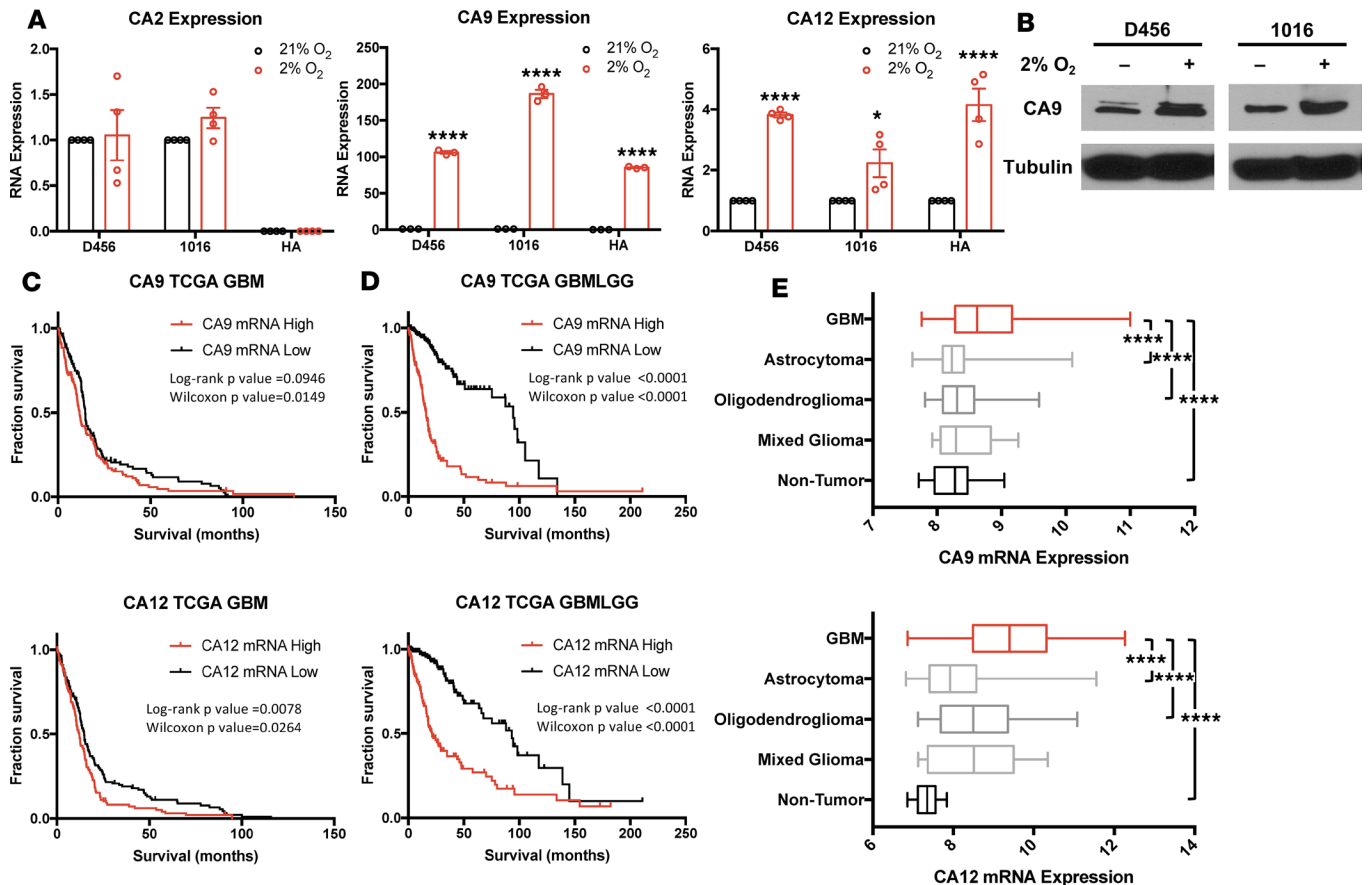


Figure 1. Carbonic anhydrase gene family expression in normal human brain and GBM patient-derived xenografts. D456 and 1016 GBM patient-derived xenografts (PDX) and human astrocytes were incubated for 72 hours in 21% or 2% O₂ and harvested for RNA. (A) Fold change in mRNA expression of carbonic anhydrase family members. * $P < 0.05$, **** $P < 0.0001$, ANOVA comparison to normoxic controls ($n = 4$ CA2, 3 CA9, 4 CA12). (B) Increased expression of CA9 protein in D456 and 1016 PDX cells incubated in hypoxia and confirmed by Western blot. mRNA expression of CA9 and CA12 in (C) GBM and (D) all gliomas, as correlated with patient survival in The Cancer Genome Atlas database (upper and lower quartiles). (E) Expression of CA9 and CA12 in GBM and low-grade gliomas as compared with nontumor. Boxes represent the first and third quartiles; median values are represented as line in box; whiskers depict the minimal and maximal values. * $P < 0.05$, **** $P < 0.0001$, ANOVA.

that a CA9- and CA12-specific inhibitor could offer potential as an anti-GBM therapy targeting tumor microenvironmental effects, since *CA9* and *CA12* were the only carbonic anhydrases to be both induced by hypoxia and correlate with poor glioma patient prognosis.

SLC-0111 inhibits GBM growth in vitro. The first-line chemotherapy agent for treatment of GBM is TMZ, a DNA-alkylating agent. In 2005, Stupp et al. reported that addition of TMZ to radiotherapy increased median overall patient survival by approximately 2 months (12.1 months to 14.6 months) and increased the percentage of 2 year survivors from 10% to 26.5% (2). Increased sensitivity to TMZ is associated with reduced expression/increased promoter methylation of O⁶-methylguanine-DNA methyltransferase (*MGMT*), which reverses TMZ-induced guanine methylation that would otherwise be highly toxic. Combinatorial approaches to further augment the efficacy of TMZ against GBMs are therefore of great potential benefit. Based on our interest in targeting tumor microenvironmental effects, we performed an initial screen of TMZ treatment alone or in combination with the CA9- and CA12-specific inhibitor SLC-0111 or the broader carbonic anhydrase inhibitors methazolamide and topiramate (Supplemental Figure 3, A and B). Our results suggested only the addition of SLC-0111 to TMZ treatment had a significant antigrowth benefit in D456 and 1016 GBM PDX cells, which both express minimal levels of *MGMT* (Supplemental Figure 3C). We therefore focused our investigation on the effect of SLC-0111 alone or in combination with TMZ. Monotherapy with SLC-0111 or TMZ significantly decreased the growth of D456 and 1016 GBM PDX cells in normoxia (Figure 2A) or

hypoxia (Figure 2B). In contrast, SLC-0111 alone had no effect on astrocyte growth, but TMZ did cause growth inhibition (Figure 2, A and B). The combination of SLC-0111 and TMZ significantly decreased GBM PDX cell growth in comparison to either drug alone but did not increase the toxicity of TMZ against astrocytes (Figure 2, A and B). Visualization of GBM cells using light microscopy confirmed differences in cell growth with SLC-0111 and TMZ combinatorial treatments (Figure 2C).

To further characterize genomic alterations that may affect SLC-0111 efficacy, we tested the combinatorial therapy on U87 parental cells that are *TP53* wild-type or derivative cells that we generated to be *TP53*-knockout cells using CRISPR (Supplemental Figure 4). Similar to our prior findings, U87 parental cells were highly sensitive to the antigrowth effects of SLC-0111 (Supplemental Figure 4A). While U87 *TP53*-knockout cells remained significantly growth inhibited with the SLC-0111 and TMZ combination (Supplemental Figure 4B), the extent of the change in cell growth was reduced (8- vs. 2-fold reduction in the wild-type and *TP53*-knockout cells in hypoxia, for example). Thus, *TP53* status could affect but not eliminate the efficacy of the SLC-0111 combinatorial treatment.

As the prior cells utilized for in vitro experiments were growth inhibited by TMZ, we also examined the effect of SLC-0111 on U251 cells generated to be resistant to TMZ or their parental counterpart (35). We again found that there was a benefit for addition of SLC-0111 to TMZ in the parental U251 cells (Supplemental Figure 5). In U251 TMZ-resistant cells (UTMZ), however, there was no significant growth inhibitory effect of SLC-0111 alone or in combination with TMZ (Supplemental Figure 5B). These data suggested that tumors completely refractory to TMZ would not benefit from the addition of SLC-0111 alone and that additional combinatorial approaches may be needed. While we had considered a contrasting hypothesis, that SLC-0111 could be particularly efficacious in *IDH1* mutant cells that we anticipated would be highly sensitive to TMZ, we did not observe a strong benefit for the addition of SLC-0111 to TMZ treatment in a *IDH* mutant BTIC line (Supplemental Figure 6). Together, our in vitro data suggest that SLC-0111 combinatorial therapy may be most efficacious in TMZ-responsive TP53-expressing tumors and that SLC-0111 is unlikely to antagonize TMZ effects in GBMs or increase the toxicity of TMZ against astrocytes.

The combination of SLC-0111 and TMZ reduces GBM cell proliferation and increases cell death in association with increased DNA damage. To identify potential mechanisms for the decreased growth with the SLC-0111 and TMZ combination, we next utilized EdU incorporation to characterize the cell cycle of GBM PDX cells after at least 5 days of treatment. Although the exact pattern of cell cycle alterations was not identical between the xenografts, the combination of SLC-0111 and TMZ consistently reduced the percentage of cells in the proliferative S phase (Figure 3, A and B, and Supplemental Figure 7). There was also a marked increase of cells in the sub-G₁ phase, indicating increased cell death in response to combinatorial treatment in D456 and 1016 cells. Interestingly, the combination also produced an increase in the proportion of cells in the G₂ phase as compared with TMZ alone (Figure 3, A and B, and Supplemental Figure 7), suggesting that G₂ arrest is enhanced by the addition of SLC-0111. Finally, the proportion of polyploid cells was significantly higher in cells treated with the combination therapy, most likely as a response to insufficient DNA repair and mitotic catastrophe.

We next sought to further characterize whether the decreased growth was due to alterations in DNA damage responses. The comet assay technique was employed to visualize and quantify tail moments on cells treated as above over a time course (Figure 3, C and D, and data not shown). TMZ alone or in combination with SLC-0111 caused DNA damage, as indicated by increased tail moments that were maintained for a longer period of time in the presence of SLC-0111. For example, cells treated with the combinatorial therapy still had significantly higher amounts of tail moments 48 hours after treatment, while cells treated with TMZ alone had returned to baseline (Figure 3, C and D). These data suggest an impaired ability to repair damaged DNA in the presence of SLC-0111. We also observed upregulated γ H2AX, a DNA double-strand break marker, in cells treated with both SLC-0111 and TMZ after 7 hours, confirming higher DNA damage (Figure 3E). Together, our data suggest that the addition of SLC-0111 to TMZ increases DNA damage to contribute to reduced glioma growth.

SLC-0111 and TMZ combination treatment influences intracellular pH and metabolism. CA9 is thought to regulate intracellular pH and metabolic adaptation to hypoxia, and therapy-mediated disruption of the altered pH balance (intracellular pH > extracellular pH) of cancer cells has been proposed to inhibit protumorigenic microenvironmental effects in solid tumors. Using the pH indicator carboxy-SNARF-1, we measured the intracellular pH of 1016 GBM PDX cells after 48 hours of treatment with vehicle or with each drug alone or in combination. While SLC-0111 treatment alone did not have a significant affect at this time point, the addition of SLC-0111 to TMZ shifted intracellular pH toward a more acidic state (Supplemental Figure 8A).

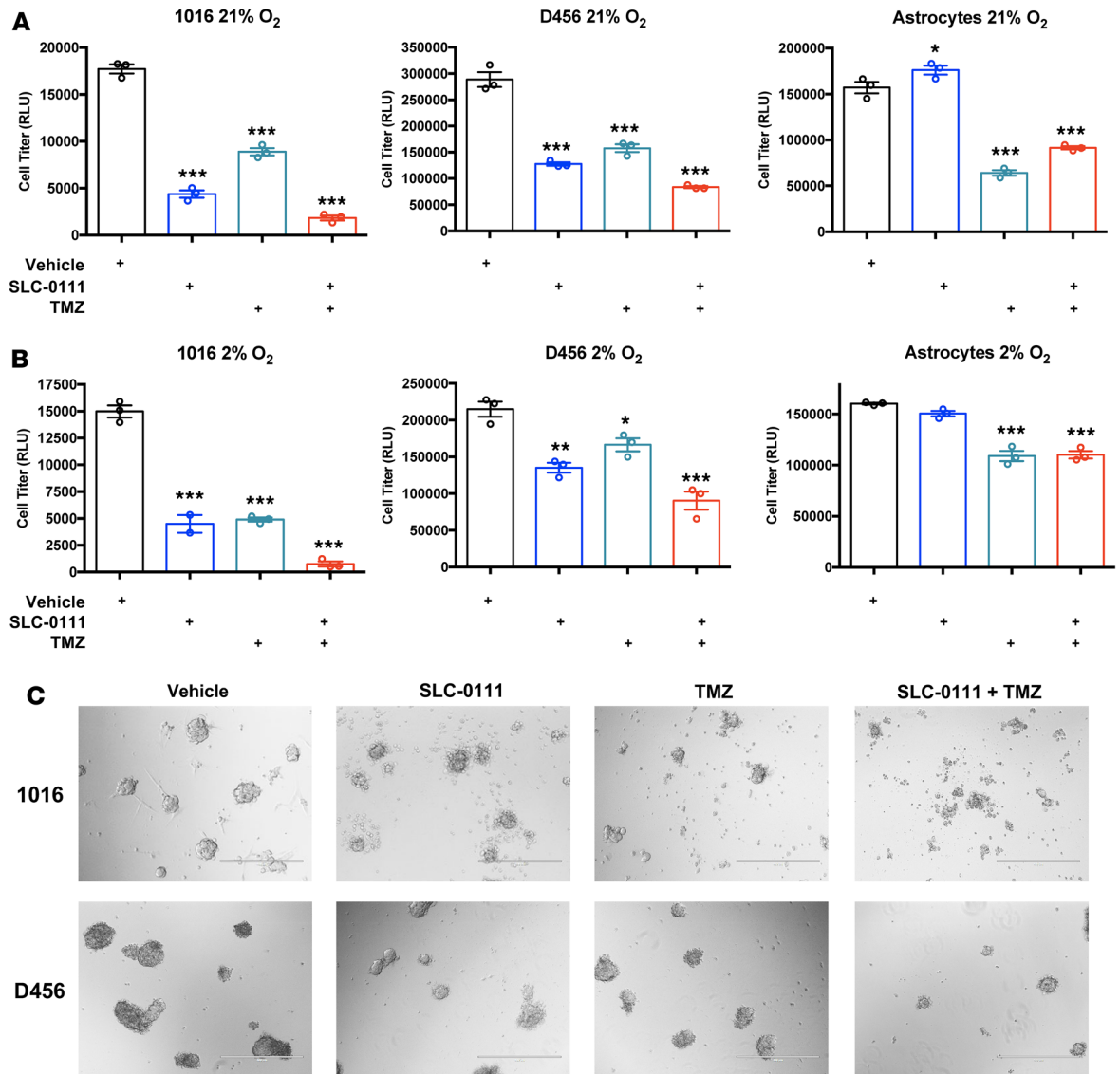


Figure 2. SLC-0111 and TMZ inhibit GBM growth in vitro. D456 or 1016 GBM PDX cells and human astrocytes were incubated for 7 days at 20% O₂ (A) or 2% O₂ (B) and treated with 50 μM SLC-0111 and 120 μM TMZ separately or in combination. Cell growth was determined using cell titer assay (*n* = 3). (C) Micrographs (original magnification, ×20) of D456 and 1016 tumorspheres after treatments in A and B. **P* < 0.05, ***P* < 0.01, ****P* < 0.001, ANOVA comparison to the vehicle.

The effect of SLC-0111 and TMZ combinatorial therapy on cellular metabolism was next determined through analysis of the metabolome of subcutaneous tumors harvested from mice treated via oral gavage. Consistent with classic studies, a Warburg-like effect characterized by aerobic glycolysis has been shown in solid tumors, including GBMs (36–38). Metabolites associated with both glycolysis and the TCA cycle have been identified as either cancer markers or oncometabolites (38). Here, we saw significant reductions in several key metabolites necessary to sustain flux through the TCA cycle when SLC-0111 is used in combination with TMZ that are not observed when the drugs are used in isolation (Figure 4A). For example, acetyl-CoA (Figure 4B), fumarate (Figure 4C), and its precursor argininosuccinate (Figure 4D) as well as pyruvate are reduced following treatment with SLC-0111 and TMZ (Figure 4). Consistent with these data, intracellular and extracellular lactate are increased (Supplemental Figure 8E). This would be expected to suppress bioenergetic capacity of the cell and decrease metabolic intermediates needed for cell growth. Supporting this conclusion, we also noted a depletion of alanine (Figure 4E) and tyrosine and accumulation of the amino acids serine (Supplemental Figure 8B), leucine (Supplemental Figure 8C), and proline (Figure 4A). Serine is generally thought to promote

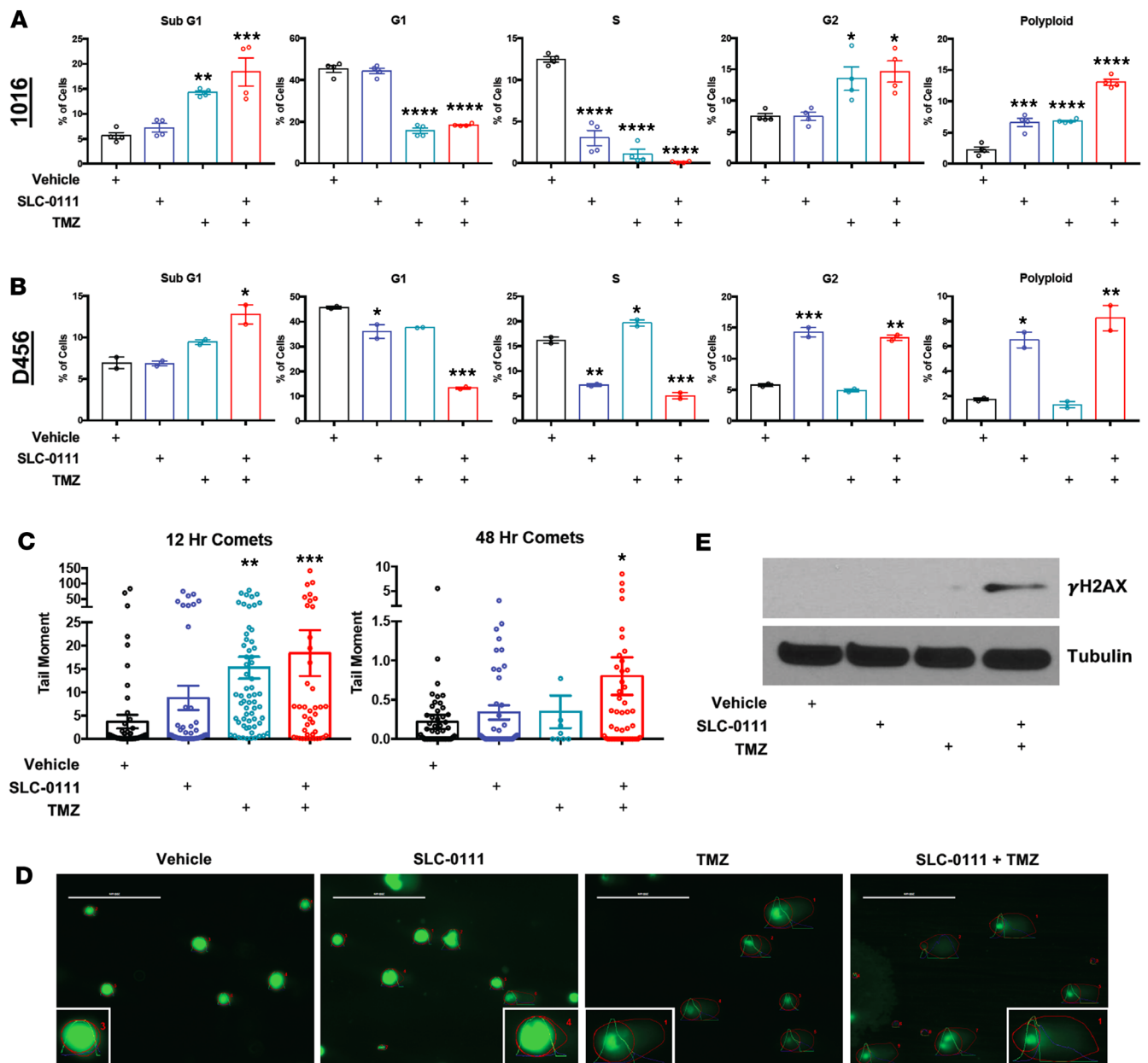


Figure 3. SLC-0111 and TMZ alter GBM cell cycle and DNA repair. 1016 and D456 GBM PDX cells were treated with SLC-0111 and/or TMZ and incubated in 2% O₂ for 7 days. Cell cycle data were quantified and graphed as cell fraction in sub-G₁, G₁, S, or G₂ phase and polyloid for 1016 (A) and D456 (B) cells ($n = 4$). (C) Representative quantification of tail moments from 3 independent experiments in 1016 GBM PDX cells treated with drug for 12 and 48 hours using a comet assay depicting extent of DNA damage. (D) Representative images from 12-hour analysis in C (original magnification, $\times 20$; $\times 40$ [inset]). (E) Western blot depicting DNA double-strand break marker γ H2AX from 1016 GBM PDX cells after 7 hours of treatment. * $P < 0.05$, ** $P < 0.01$, *** $P < 0.001$, **** $P < 0.0001$, ANOVA comparison to the vehicle.

tumor growth, but the elevation here may reflect a buildup due to reduced consumption for alanine, the production of which requires pyruvate (Figure 4A). Similarly, leucine increases could result from changes in protein synthesis or breakdown or even altered fatty acid synthesis, since leucine is converted to acetyl-coA, which is significantly reduced with the combinatorial therapy (Figure 4A).

Our *in vivo* results strongly suggest a broad suppression in the metabolic plasticity necessary to sustain tumor growth with SLC-0111 and TMZ dual therapy. It is important to note, however, that our *in vitro* results suggest that there may be an adaptive selection for surviving glycolytic cells over time. Using extracellular flux (XF) assays conducted in low buffering capacity media in hypoxia, we monitored metabolic output after treatment over a time course. We indirectly measured glycolytic activity

via extracellular acidification rate and aerobic respiration via oxygen consumption rate. After plotting these data on an energetic map to compare the time points of treatment, we discovered that, in the combination treatment of SLC-0111 and TMZ, the rate of cellular glycolysis is uniquely increased by 24 hours after treatment and that an elevated glycolytic state is maintained through the 48 hours after treatment (Supplemental Figure 8 and data not shown). Protein content assays used to correct for differences in cell number demonstrated that cells were sensitive to SLC-0111-mediated growth inhibition under the XF experimental conditions (data not shown). As noted above, intracellular and extracellular lactate production were also significantly increased only with combinatorial treatment when data were corrected for the reduced cell number (Supplemental Figure 8E).

Addition of SLC-0111 to TMZ treatment reduces CD133 expression and neurosphere formation. Treatment of GBM xenografts with radio- and chemotherapy has been previously shown to enrich for BTIC markers, and we confirmed via flow cytometry elevation of the CD133⁺ fraction in xenograft-derived GBM cells treated with TMZ (Figure 5A). While we did not observe significant changes in the percentage of CD133⁺ cells with SLC-0111 treatment alone, SLC-0111 significantly blunted the elevation in stem cell marker expression induced by TMZ treatment (Figure 5A and Supplemental Figure 9). In addition, expression of the astrocyte lineage differentiation marker glial fibrillary acidic protein (*GFAP*) was significantly elevated when SLC-0111 was used in combination with TMZ (Figure 5A). To determine the effectiveness of this therapy on BTICs versus differentiated cells, we also performed cell growth experiments on 1016 and D456 cells, sorted based on expression of CD133. We observed that in both 1016 and D456 cells, the BTIC (CD133⁺) fraction was more sensitive to the combinatorial treatment than the non-BTIC (CD133⁻) fraction (Figure 5B). As the ability for GBM tumor cells to form neurospheres in a sphere formation assay has been shown to be an indicator of self-renewal, D456 and 1016 cells pretreated with SLC-0111 alone and in combination with TMZ were subsequently plated in the absence of any drug to calculate the percentage of functional BTICs remaining (Figure 5C). Extreme limiting dilution analysis determined that SLC-0111 in combination with TMZ significantly decreased the percentage of BTICs in cells isolated from both xenografts (Table 1). These data demonstrate that the efficacy of TMZ can be enhanced through addition of SLC-0111, due, in part, to a reduction in BTIC enrichment after chemotherapy.

Differentiation therapy is enhanced by SLC-0111 addition. While the focus of this study involves using SLC-0111 in combination with TMZ because it is standard of care for GBM patients, we also sought to explore the potential benefits of alternative combinatorial approaches. Differentiation therapy, to either decrease cell proliferation or decrease BTIC maintenance, is one strategy that has been proposed for GBM therapy. Bone morphogenetic protein (BMP) treatment was shown to extend survival of mice bearing GBM xenografts due to increased differentiation of BTICs toward an astrocyte lineage (39). We therefore determined if SLC-0111 could be effective in combination with BMP. Similar to previously published data, we found that BMP4 inhibited the growth of D456 and 1016 PDX cells after 7 days (Supplemental Figure 10). We also verified our prior findings that SLC-0111 alone was sufficient to decrease GBM growth in vitro (Supplemental Figure 10). When SLC-0111 was used in combination with BMP4, GBM PDX cell growth was significantly inhibited in comparison to the vehicle or either treatment alone (Supplemental Figure 10A). Importantly, astrocytes were unaffected by any treatment alone or in combination (Supplemental Figure 10B). These data suggest that combinatorial approaches involving SLC-0111 beyond TMZ, and particularly those that promote differentiation, may be effective against GBM and are worth further investigation.

Combinatorial treatment delays GBM growth in vivo. Our in vitro data strongly suggested there could be a benefit for addition of SLC-0111 to TMZ therapy for GBM treatment in vivo. We investigated this possibility by subcutaneously implanting GBM PDX cells into athymic nude immunocompromised mice. After tumor establishment, mice were treated with vehicle, SLC-0111 or TMZ alone, or SLC-0111 and TMZ in combination. SLC-0111 treatment alone was ineffective at delaying tumor growth in vivo in comparison to the vehicle control. However, the combination of SLC-0111 and TMZ delayed tumor recurrence more than either monotherapy (Figure 6A) with complete regression in two mice. To further investigate this in a model system that would mimic the recurrent GBMs likely to be first enrolled in clinical trials, we engrafted 1016 GBM PDX cells intracranially to form orthotopic xenografts and treated mice as described above. Although SLC-0111 was not sufficient to improve survival alone, TMZ alone and in combination with SLC-0111 significantly improved survival (Figure 6B). 130 days after implantation, median survival for the TMZ treatment group was 76 days, while median survival could not be determined for the combination

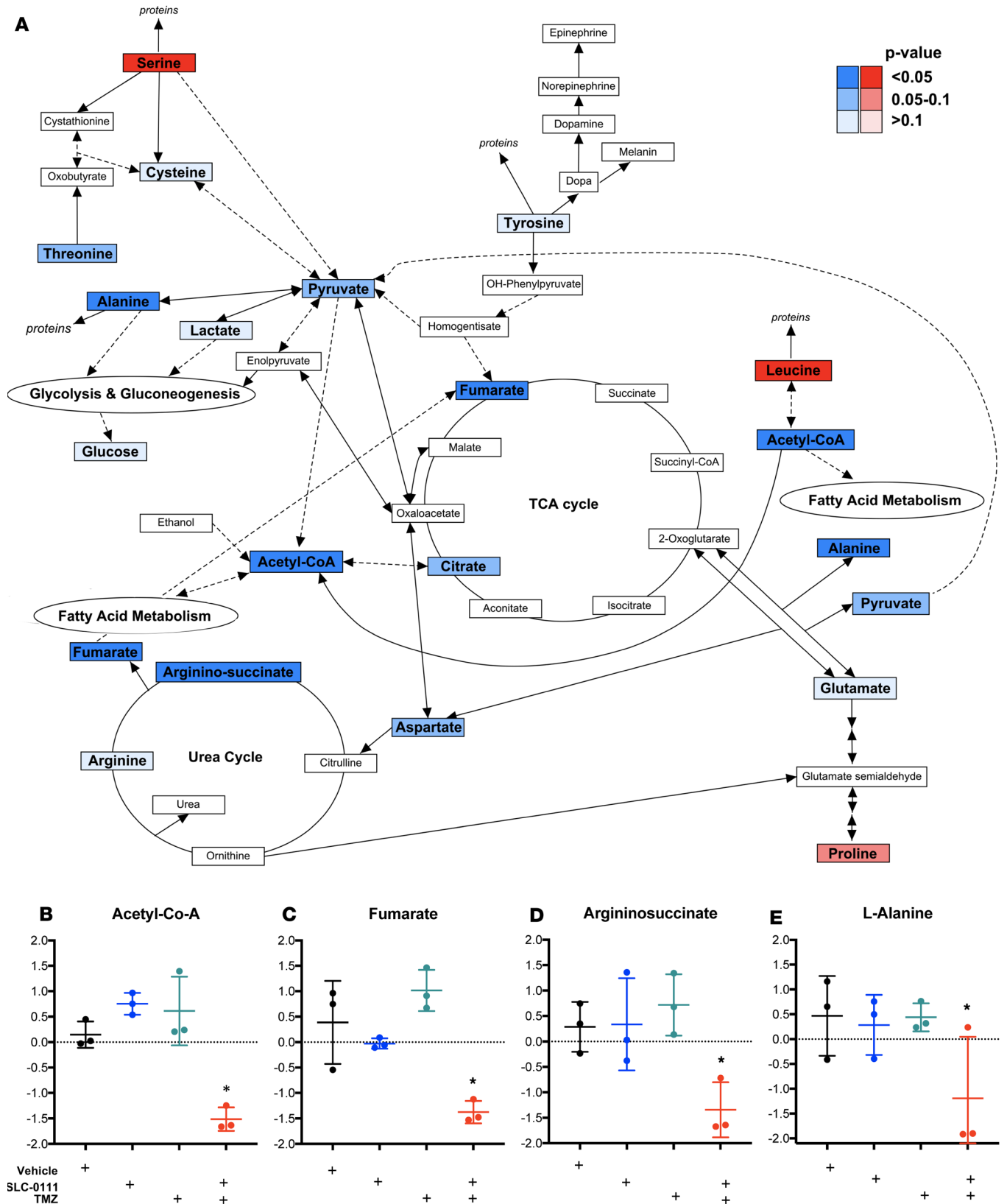


Figure 4. Influence of SLC-0111 and TMZ combinatorial therapy on metabolism. Subcutaneous 1016 GBM PDX cells were treated with vehicle or SLC-0111 in the presence or absence of TMZ, and treated tumors were snap frozen in liquid nitrogen. Metabolomics processing and analysis performed on tissue samples with a sample set of 3 with technical replicate. **(A)** Pathway map indicating decrease (blue) or increase (red) in metabolites when treated with SLC-0111 and TMZ combinatorial therapy (ANOVA overall comparison). Box plots demonstrate decreased **(B)** acetyl-CoA, **(C)** fumarate, **(D)** argininosuccinate, and **(E)** alanine with combinatorial therapy. * $P < 0.05$, ANOVA comparison to vehicle.

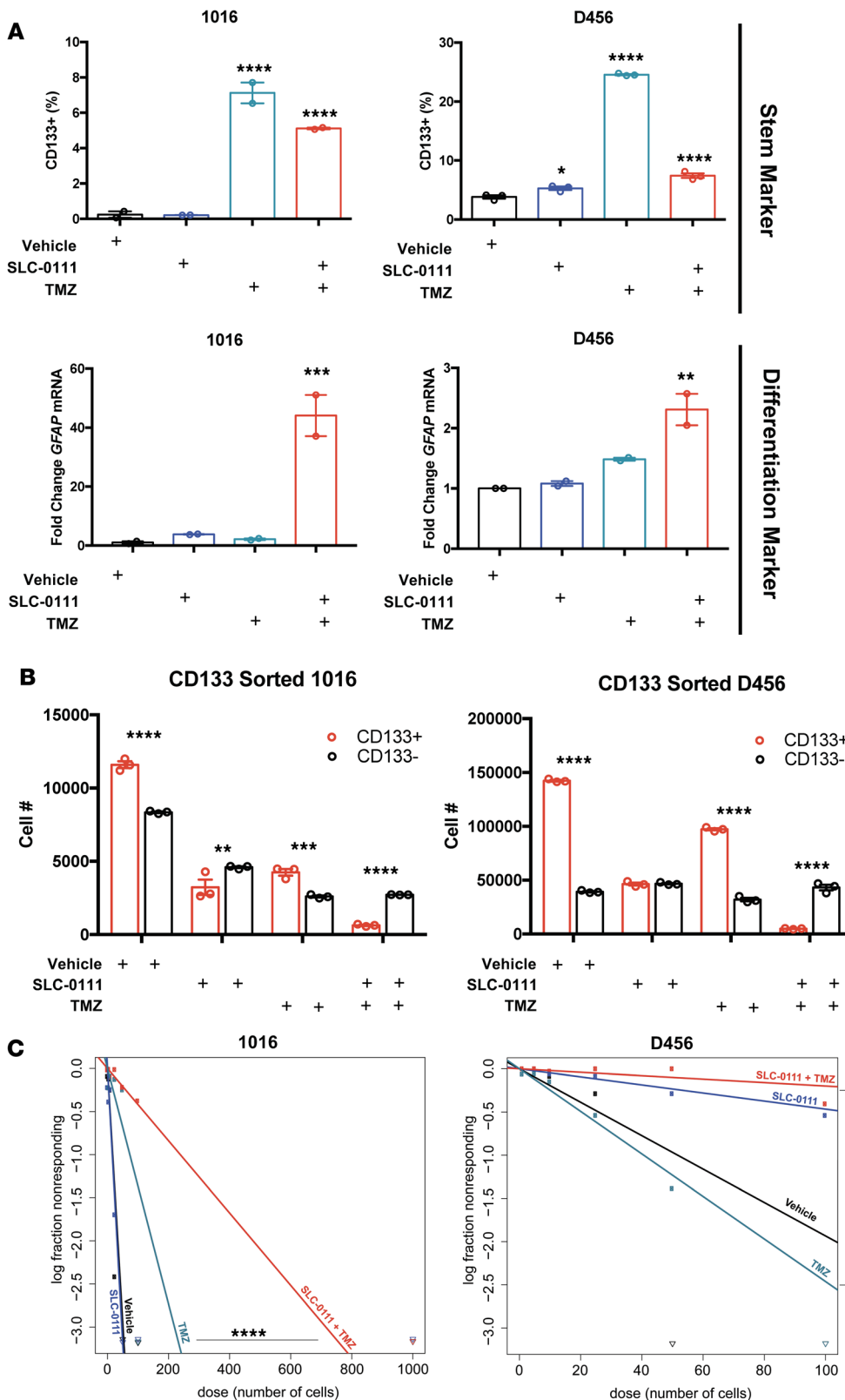


Figure 5. SLC-0111 and TMZ combinatorial therapy reduces BTIC marker expression and neurosphere formation capacity. Bulk tumor cells isolated from D456 and 1016 PDX cells were treated with SLC-0111, TMZ, or DMSO and incubated in 2% O₂ for at least 5 days. (A) Flow cytometry analysis of CD133 cell surface expression as a marker of stem cells (*n* = 3) and GFAP mRNA expression as a marker of differentiated cells (*n* = 2). (B) Cell growth measured via cell titer assay of CD133-sorted 1016 and D456 GBM PDX cells treated with drug for 7 days (*n* = 3). (C) Representative analysis from 3 independent experiments analyzing neurosphere formation after treatment with SLC-0111, TMZ, or DMSO for 7 days. Cells were plated for neurosphere formation under standard conditions in the absence of drug. **P* < 0.05, ***P* < 0.01, ****P* < 0.001, *****P* < 0.0001, ANOVA.

(Table 2). Analysis of tumor sections from treated mice demonstrated that expression of the BTIC marker SOX2 was decreased with the addition of SLC-0111 to TMZ therapy (Figure 6C), confirming our in vitro result that SLC-0111 decreased BTIC enrichment after TMZ treatment. These data demonstrate that there is a significant in vivo benefit of addition of SLC-0111 to TMZ for treatment of GBM.

Table 1. Stem cell frequency in sphere formation assay

| D456 | | 1016 | |
|----------------|------------------|----------------|------------------|
| Treatment | 1/stem cell freq | Treatment | 1/stem cell freq |
| Vehicle | 51.7 | Vehicle | 17.8 |
| SLC-0111 | 214.5 | SLC-0111 | 16.5 |
| TMZ | 40.6 | TMZ | 77.1 |
| SLC-0111 + TMZ | 503 | SLC-0111 + TMZ | 251.3 |

Data in Table 1 correspond to that in Figure 4. Extreme limiting dilution analysis of sphere formation assays in D456 and 1016 cells pretreated with the indicated drugs demonstrates decreased stem cell frequency with SLC-0111 and TMZ combinatorial therapy. 1/stem cell freq, statistical frequency of stem cells in bulk tumor cells.

Discussion

Current treatment strategies for GBM allow for an approximately 14-month median survival time after diagnosis in patients (2, 40, 41). While this is an abysmal outlook for patients many efforts are underway to improve survival, with recent data suggesting promising results with novel combinatorial therapies (42, 43). TMZ is the current standard-of-care chemotherapy agent employed in the clinic for GBM patients, but its effect on median patient survival is relatively small (increased 2 months). We believe that our data strongly suggest that a strategy to target a tumor-specific carbonic anhydrase, CA9, will improve TMZ efficacy and potentially improve patient outcomes. The combination of SLC-0111 and TMZ may provide a benefit through several potential mechanisms, including reduced GBM cell growth, sustained DNA damage, inhibition of BTIC enrichment after chemotherapy, suppression of GBM cellular bioenergetic capacity, and decreased metabolic intermediates. In addition, it appears that resistance to TMZ involves a selection for more aerobic metabolism (44), and it therefore follows that a greater suppression of metabolic plasticity in the tumor at the time of initial therapy would be beneficial. However, we recognize there are limitations of our approach and there are alternative interpretations of our mechanistic data. Changes in cell growth and viability induced by SLC-0111 and TMZ treatment may lead to metabolic changes rather than directly modifying the pathways. Although SLC-0111 has high affinity for CA9, we also cannot eliminate the possibility that off-target effects contribute to the tumor growth inhibition observed. Further experiments with additional time points or genetic targeting may help to clarify the exact mechanisms through which the bioenergetic and metabolic changes induced by SLC-0111 in combination with TMZ are significantly greater than either drug alone. As TMZ can induce a transient decrease in intracellular pH that recovers by 24 hours (45), we speculate that SLC-0111 may further shift that balance and maintain the decrease in pH. If TMZ could be utilized at lower doses with equivalent effects on GBM growth inhibition when used with SLC-0111, TMZ side effects could also be reduced. This notion is supported by the minimal effect of SLC-0111 on nonneoplastic human astrocytes.

TMZ is most effective in a subset of GBM patients who do not express MGMT, as it reverses guanine methylation that causes DNA damage (46). *MGMT* expression is highly associated with promoter methylation, making *MGMT* methylation status a potential biomarker for TMZ sensitivity (33). In the BTICs used here, we observed very low MGMT protein expression and we determined that UTMZ cells were not sensitive to combination therapy with SLC-0111 and TMZ. However, patients are treated with both TMZ and IR, and we have not yet tested the efficacy of SLC-0111 in this combinatorial approach. Our results with BMP4 as a differentiation therapy in combination with SLC-0111 do suggest that there could be benefit for alternative combinatorial approaches, even when TMZ-based approaches are no longer viable. We also recognize that there is a strong potential for differences in therapeutic efficacy of small-molecule inhibitors between in vitro and in vivo models, and we have observed this for SLC-0111 monotherapy as well. Our data highlight the importance of improving our in vitro conditions to better model physiologic microenvironments to hopefully improve prediction of in vivo efficacy and metabolic alterations. Taking these current limitations into account, we believe it is critical to further evaluate the efficacy of TMZ and irradiation in the presence and absence of SLC-0111 in vivo in multiple models, including those with *IDH* mutation, *TP53* homozygous deletion, or high MGMT expression. This would be informative for defining subsets of glioma patients most likely to benefit from SLC-0111 treatment. Improvements to in vivo combinatorial approaches could also be achieved through pharmacodynamic and pharmacokinetic studies of SLC-0111

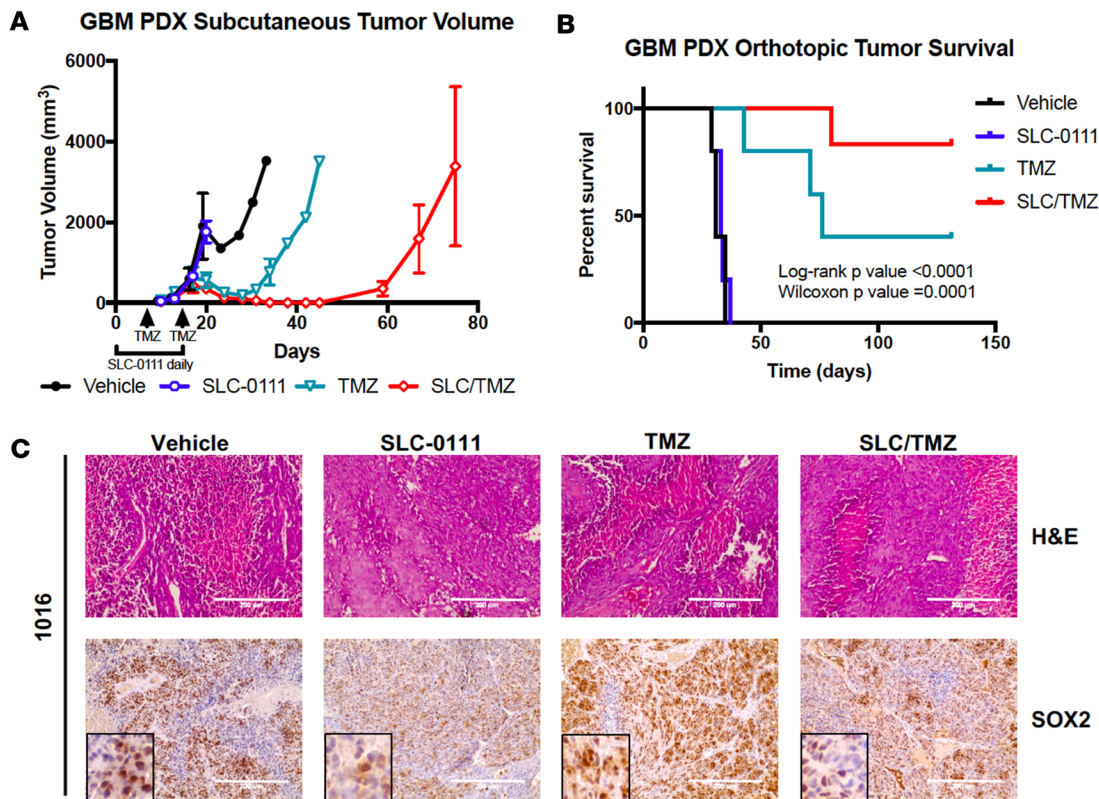


Figure 6. SLC-0111 and TMZ combinatorial treatment delays tumor growth in vivo. 1016 GBM PDX cells were implanted subcutaneously ($n = 3-4$) (A) or intracranially ($n = 5-6$) (B) into mice, which were treated via oral gavage with SLC-0111 for 14 days alone or SLC-0111 in combination with TMZ once a week. Caliper measurements were used to determine the displayed subcutaneous tumor volume in A. (B) Mice bearing orthotopic GBM tumors were monitored and sacrificed after developing neurological signs. (C) Immunohistochemistry was performed in tumors harvested 72 hours after a single TMZ treatment and daily SLC-0111 treatment (original magnification, $\times 20$; $\times 40$ [inset]).

levels to identify the proportion of SLC-0111 in the brain and the time at which brain levels are maximal.

Our treatment strategy utilizes SLC-0111 rather than other carbonic anhydrase inhibitors because we wished to exploit the wider therapeutic window for CA9 targeting. CA9 is highly expressed in GBM PDX cells subjected to hypoxic conditions and has restricted expression in nonneoplastic tissues, suggesting the potential to inhibit tumor microenvironmental effects with minimal toxicity through CA9 inhibition. A possible added benefit to using SLC-0111 is the ability of this small-molecule inhibitor of CA9 to also target CA12. We evaluated *CA12* expression with GBM patient survival and found that this gene may also be important for GBM tumorigenicity (Figure 1, C–E), but a role for CA12 has not been well investigated in cancers.

In addition, we also acknowledged that other carbonic anhydrase inhibitors do not display high specificity. For example, methazolamide inhibits CA1, CA2, and CA4, and topiramate inhibits voltage-gated sodium channels and as well as kainite receptors and carbonic anhydrases. When we evaluated the ability of topiramate to inhibit GBM growth in the presence or absence of TMZ, we noted no additional benefit (Supplemental Figure 3), but a recent study indicated that topiramate treatment decreased intracellular pH in U87 GBM cells in vivo (47). Antiepileptic drugs including topiramate are often used for treatment of tumor-associated epilepsy, but results to determine direct efficacy against GBM cell growth in vitro have been mixed (48, 49). Although several antiepileptic drugs have not demonstrated significant improvements in overall survival (50), our data suggest that further clinical evaluation of those with carbonic anhydrase inhibitor function is warranted.

Carbonic anhydrases work in conjunction with bicarbonate transporters to modulate the tumor cell pH gradient by modulating the number of protons and bicarbonate molecules inside and outside the cell. A recent report demonstrated that genetic targeting of sodium bicarbonate transporters with siRNA could decrease the growth of U87 GBM cells in vitro and in vivo (51). These data suggest that it will be important to consider the entire carbonic anhydrase–bicarbonate transporter system and its effects on TMZ treatment in the future. Furthermore, dual targeting of GBM that expresses bicarbonate transporters with SLC-0111 could provide an antitumor effect in the absence of any chemotherapy and should be considered. The recent finding that there is a strong association between bicarbonate and amino acid transporters with CA9 also suggests additional mechanisms through which CA9 inhibition could alter metabolism (52).

Table 2. Median survival for 1016 orthotopic tumors

| | Vehicle | SLC-0111 | TMZ | SLC + TMZ |
|---------------------|---------|----------|-----|-----------|
| Median survival (d) | 31 | 33 | 76 | N/A |
| Incidence (n) | 5 | 5 | 3/5 | 1/6 |

Data in Table 2 correspond to that in Figure 6. Median survival in athymic nude mice implanted with 1016 GBM and treated with vehicle, SLC-0111, TMZ, or SLC-0111 and TMZ in combination.

We used SLC-0111 to target CA9 in BTICs isolated from both an aggressive pediatric xenograft (as shown using D456 cells) and a recurrent adult GBM xenograft (as shown using 1016 cells) and demonstrated a consistent decrease in BTIC growth and enrichment when used in combination with TMZ. Clinical trials in GBM often comprise patients with a tumor recurrence, and we have demonstrated *in vivo* efficacy for SLC-0111 with TMZ in a recurrent GBM. Therefore, our data strongly suggest the translational potential of SLC-0111 for GBM therapy.

Methods

Xenografts and cell lines. GBM PDX D456 (pediatric) cells were obtained from Darell Bigner at Duke University in Durham, North Carolina, USA, and 1016 (recurrent adult) cells were obtained from the University of Alabama at Birmingham Brain Tumor Core Facility. IDH mut HK-322 BTICs were obtained by KPB from Harley Kornblum at the University of California, Los Angeles, in Los Angeles, California, USA. The PDXs were passed through mice as subcutaneous tumors and dissociated using Worthington's Biochem Papain Dissociation System (LK003150) and GBM cells were propagated in Gibco phenol red-free DMEM/F12 containing 2.5 mM L-glutamine and 17.5 mM glucose and supplemented with B27 equivalent-Gem 21 (Gemini Biosciences), 20 ng/ml epidermal growth factor and fibroblast growth factor basic, 1% sodium pyruvate, and 1% penicillin/streptomycin. Immortalized human astrocytes (HAs) were obtained from the University of Alabama at Birmingham Brain Tumor Core Facility. U87 parental cells were purchased from ATCC, and U87 p53-knockout cells were generated via CRISPR. 1 µg plasmid-expressing sgRNA specific for p53 and Cas9 (provided by Xinbin Chen of the University of California at Davis in Davis, California, USA) was used to transfect U87 cells using Fugene 6 (Promega). At 24 hours after transfection, cells were seeded at 1 cell/well per 96-well plate and grown in complete media containing 0.5 µg/ml puromycin. Clones were successively amplified and screened for loss of TP53 expression by treating cells with camptothecin (damages DNA) for 24 hours and evaluated by Western blot. U251 parental or TMZ-resistant UTMZ cells were generated as previously described (35).

Reagents. SLC-0111 and TMZ, utilized for *in vitro* studies, were purchased from Selleck Chemicals and dissolved in DMSO; TMZ was administered at a concentration of 120 µM and SLC-0111 was administered at a concentration of 50 µM for *in vitro* studies. For animal administration, SLC-0111 was obtained in oral formulation from Welichem Biotech Inc. and administered to mice at a concentration of 100 mg/kg. Temodar (Merck & Company) was resuspended in Ora-Sweet (Fisher Scientific) and administered to mice at a final concentration of 100 mg/kg. BMP4 (R&D Systems) was resuspended per the manufacturer's suggestions. Carboxy SNARF-1 pH indicator, developed by Molecular Probes, was obtained from Thermo Fisher Scientific. For Western blotting, CA9 antibody was obtained from Novus Biologicals (NB100-417), tubulin antibody was obtained from MilliporeSigma (T6074), phospho-H2A.X antibody was obtained from Cell Signaling (9718), MGMT antibody was obtained from Fisher Scientific (35-7000), lamin B1 antibody was obtained from Cell Signaling (12586S), and p53 antibody was obtained from Cell Signaling (2527S). For immunohistochemistry, Sox2 antibody was obtained from BD Pharminogen (561469).

***In silico* analysis.** Correlations between patient survival and carbonic anhydrase family gene expression were plotted using Kaplan-Meier survival curves with data from the National Cancer Institute's Repository for Molecular Brain Neoplasia Data (53) and The Cancer Genome Atlas using GlioVis (32).

Carbonic anhydrase expression. D456 and 1016 GBM cells as well as immortalized human astrocytes were plated at a density of 100,000 cells per well in a 6-well plate and were cultured in normoxia (21% O₂) or hypoxia (2% O₂) after overnight recovery. GBM cells were plated on Geltrex (Thermo Fisher), a laminin-containing matrix, to prevent cells from growing as spheres and obtaining varying hypoxic zones. Cells

were collected after 3 days; RNA was isolated utilizing the illustra RNAspin Mini Kit (GE Healthcare) and converted into cDNA using iScript cDNA Synthesis kit (Bio-Rad). Basal level expression of CA2, CA4, CA6, CA9, CA12, and CA13, which have been implicated in pH regulation and/or shown to be expressed in tumors, was analyzed utilizing PrimePCR gene-specific primers (Bio-Rad), with SsoAdvanced Universal SYBR Green Supermix on the CFX Connect real-time system (Bio-Rad).

Cell growth. Cells were plated at a density of 1,000 (D456 and HA) or 2,000 (1016) cells per well in Corning black clear-bottom 96-well plates. Cells recovered overnight and were then incubated in normoxia (21% O₂) or hypoxia (2% O₂) for a total of 7 days, with treatment on day 1 and day 3 with 50 μM SLC-0111 and 120 μM TMZ alone or in combination. For experiments with BMP, cells were treated with 50 μM SLC-0111 and 25 ng/ml BMP4 separately and in combination. On day 7, a 1:1 ratio of cell titer glo 2.0 (Promega) was added to the plate and incubated for 10 minutes, and luminescence was read on a Clarity (Bio Tek) spectrophotometer.

Comet assay. Treated GBM cells were suspended and embedded onto agarose-coated microscope slides and partially lysed so that only the nucleus remained intact. Following lysis, the slides were placed in an alkaline solution to mediate the uncoiling of DNA. After the alkaline bath, the slides were electrophoresed briefly and were then washed with neutralizing buffer, water, and finally pure ethanol to fix the DNA. The DNA was stained with SYBR Gold (Molecular Probes) and visualized using an EVOS FL inverted fluorescent microscope (Thermo Fisher). Comet tail moments were analyzed with the aid of ImageJ software (NIH).

Intracellular pH measurement. GBM cells were treated with vehicle, SLC-0111, TMZ, or SLC-0111 and TMZ in combination for 4 hours prior to flow cytometry. All cell preparations, including dye loading with SNARF-1 pH indicator (performed according to the manufacturer's instructions), single-cell dissociation, and flow buffer resuspensions, were performed in the presence of the vehicle or drugs. To generate a standard curve, cells treated with nigericin are bathed in high K⁺ buffers with set pH and stained with SNARF1. To determine the pH of the experimental samples, the results are compared to and extrapolated from the standard curve.

Metabolomic sample preparation. Tissue from 1016 GBM PDX cells implanted subcutaneously into mice and treated with vehicle, SLC-0111, TMZ, or SLC-0111 and TMZ in combination was flash frozen and placed in a Covaris tissueTUBE TT1 with a corresponding plug for homogenization of tissue under dry ice conditions. Metabolites were extracted from 50 mg homogenized frozen tissue using 1 ml of 50% cold methanol in an MP Biomedicals lysis matrix D tube and completely homogenized using the MP Fast-Prep-24 homogenizer (MP Biomedicals) for 2 cycles of 45 seconds at 6.5 M/s. The mixture was placed on a rotator at 4°C for 30 minutes followed by centrifugation at 17,500 g at 4°C for 10 minutes. The supernatant was aliquoted into 10-mg equivalents of initial tissue weight and dried down at 55°C for 60 minutes using a vacuum concentrator system (Labconco). Derivatization by methoximation and trimethylsilylation was performed as previously described (54).

GCxGC-TOFMS analysis. Samples were analyzed on a Leco Pegasus 4D system (GCxGC-TOFMS), controlled by ChromaTof 4.51.6 software (LecoUSA). Samples were analyzed as described previously (54) with minor modifications in temperature ramp. Technical replicates of each sample were analyzed in random order.

Data analysis and metabolite identification. Peak calling, deconvolution, and initial library spectral matching were performed using ChromaTof 4.51.6 software. Data were processed for export using the total ion chromatogram method within the ChromaTof 4.51.6 software for further data processing and alignment with the R2GC package (<http://www.biorxiv.org/content/early/2017/08/31/179168>). Using the output of this aligner, we identified metabolites using both a local standards library and Fiehn libraries (Leco). The optional methods in the R package utilized during alignment and peak calling are as follows: FindProblemPeaks, PrecompressFiles (similarityCutoff = 65), and Find_FAME_Standards. For ConsensusAlign, the missingValueLimit was set to 0 for later normalization of metabolites. After alignment and peak annotation, samples were initially normalized as a weighted average of the total area recognized for each sample. Using the normalized data, MetaboAnalyst 3.0 (55) was used to analyze the processed data using the initial parameters: missing value estimation, KNN estimation for missing values, normalization by sum, and autoscaling. PathViso 3 (56, 57) and adapted WikiPathways (56, 58) were used for the visualization of pathway map. *P* values were based on 1-way ANOVA results (MetaboAnalyst 3.0).

XF analysis. Cells were seeded at a density of 3×10^4 cells/well 24 hours prior to treatment with vehicle, SLC-0111, TMZ, or SLC-0111 and TMZ in combination for 4 hours or 48 hours in 2% O₂ before a mitochondrial stress test in the XF24 analyzer. MSTXF assays were performed in basal DMEM media without bicarbonate supplemented with 5.5 mM D-glucose, 1 mM sodium pyruvate, and 4 mM L glutamine at pH

7.4 under normoxic (21% O₂) or hypoxic (2 % O₂) conditions similar to our prior descriptions (59). The cells were equilibrated in a non-O₂ incubator for 1 hour before measurement of basal oxygen consumption rates and extracellular acidification rates for 6 hours. Cellular bioenergetics were measured by sequential injections of oligomycin (1 µg/ml), carbonyl cyanide-p-trifluoromethoxyphenylhydrazone (1 µM), and antimycin A (10 µM); in order to determine the role of glycolysis, 2-deoxy-D-glucose (50 mM) was injected.

BTIC marker analysis. For each of 3 separate experiments, vehicle control D456 and 1016 cells were plated in triplicate at a density of 150,000 cells in 10-cm² dishes. 300,000 D456 or 400,000 1016 cells were plated for treatment groups due to the decreased growth with addition of SLC-0111 and/or TMZ. Cells were treated as above with collection and trituration with a pipette for dissociation into single cells on day 5 or 7. Cells were then run through a 30-µm filter, and Fcr human-blocking buffer (Miltenyi) was added to each sample. CD-133 APC antibody (Miltenyi, AC133-APC) or an IgG-APC control (BD, BDB555751) was then added followed by incubation for 25 minutes in the dark at room temperature. During the last 5 minutes of incubation, sytox blue (Thermo Fisher) was added as a cell viability indicator. Cells were washed and resuspended in 300 µl DMEM/F12 media without supplements with subsequent flow cytometry analysis.

Neurosphere formation. D456 and 1016 cells were plated and treated as indicated for stem cell marker analysis. To calculate the percentage of BTICs remaining after treatment, vehicle- or inhibitor-treated cells were dissociated using StemPro Accutase (Thermo Fisher) and plated in serial dilutions from 1–1,000 cells. Cells were plated in a clear flat-bottom 96-well plate (Corning) in BTIC media in the absence of any drug or vehicle. Plates were incubated under hypoxia for 10–14 days and were then analyzed for formation of spheres. Statistical differences were calculated using extreme limiting dilution analysis (60).

Cell cycle analysis. 1016 cells were plated in duplicate at a density of 200,000 cells, D456 cells were plated in duplicate at a density of 150,000 cells in 6-well plates, and then cells were incubated in 2% O₂ as indicated above. Following the second treatment, cells were expanded to a 60-mm² dish. Samples were harvested and stained with PI or processed using Thermo Fisher's Click-It Plus EdU Pacific Blue Flow Cytometry Assay Kit (C10418). Experiments were repeated in triplicate.

In vivo determination of GBM growth. For subcutaneous tumor formation, homozygous CrI:NU(N-Cr)-Foxn1tm athymic nude female mice bred from Charles River strains 490 (homozygous) and 491 (heterozygous) were subcutaneously injected with 500,000 1016 cells in the right flank to establish xenografts. Tumors were grown for 10 days, and tumor-bearing mice were then randomly placed in 4 different treatment groups (vehicle control, SLC-0111 alone, TMZ alone, or SLC-0111 and TMZ). For orthotopic tumor implantation, 1,000 cells were injected intracranially and tumors were established for 10 days. Mice were treated via oral gavage at a concentration of 100 mg/kg SLC-0111 or vehicle control daily for 14 days. Concurrently, mice also received 100 mg/kg TMZ (once every 7 days over 14 days) by oral gavage. Mice were weighed and tumors measured 3 times per week. As determined by tumor burden or development of neurologic signs because there was no decrease in mouse weight, subcutaneous tumors or brains were removed, fixed in formalin, and stained for H&E. In a separate experiment, subcutaneous tumor-bearing mice were treated short term (total of 48 hours) with the amounts of vehicle, SLC-0111, and/or TMZ indicated above and tumors were harvested, fixed in formalin, stained for H&E, and evaluated for SOX2 expression via immunohistochemistry.

Statistics. All experiments were repeated in triplicate unless otherwise indicated in figure legends. All statistics were performed with GraphPad Prism version 7 unless otherwise noted. One-way ANOVA and multiple 2-tailed *t* tests were performed with Sidak's correction for multiple comparisons. Error bars are displayed as mean ± SEM. A *P* value of less than 0.05 was considered significant.

Study approval. All animal studies have been approved by the University of Alabama at Birmingham IACUC. All PDXs have been deidentified and approved for use as nonhuman subjects by the University of Alabama at Birmingham IRB.

Author contributions

NHB and KW designed the studies, conducted experiments, acquired and analyzed data, and wrote the manuscript. JF, GAB, RS, AA, SES, CJL, ANT, and EG acquired and analyzed data for figures in the manuscript. JRH, BN, MOB, and GYG helped with analyzing data and reviewing the manuscript. PCM, BN, CG, SN, KP, EEB, VDU, BX, SJC, and SD provided critical resources and technical expertise and helped to review manuscript. ABH conceived of the study, provided reagents, designed experiments, analyzed data, and wrote the manuscript.

Acknowledgments

This work was supported by NIH grants F31 CA200085, R21NS096531, and R01 CA151522; the South-eastern Brain Tumor Foundation; the University of Alabama at Birmingham Brain Tumor SPORE (P20 CA151129) Career Development Award; a pilot award from the University of Alabama at Birmingham-HudsonAlpha Center for Genomic Medicine; and startup funds from the University of Alabama at Birmingham (to ABH). These startup funds include contributions from the Department of Cell, Developmental and Integrative Biology, the Comprehensive Cancer Center, the Civitan International Research Center for Glial Biology in Medicine, the Center for Free Radical Biology, and the Neuro-Oncology Brain SPORE. Additional support was provided by NIH grants R21NS100054 and R01CA160821 (to CG), R01CA138517 (to SN), S10RR027822-01 (Targeted Metabolomics and Proteomics Core), P30 NS47466 (University of Alabama at Birmingham Neuroscience Molecular Detection Core), and P30 AI027767 (Center for AIDS Research Flow Cytometry Core). The authors would like to thank Landon Wilson and Steve Barnes from the Targeted Metabolomics and Proteomics Core.

Address correspondence to: Anita B. Hjelmeland, Department of Cell, Developmental and Integrative Biology, University of Alabama at Birmingham, THT 948, 1900 University Boulevard, Birmingham, Alabama 35294, USA. Phone: 205.996.4596; Email: hjelmea@uab.edu.

- Louis DN, et al. The 2007 WHO classification of tumours of the central nervous system. *Acta Neuropathol.* 2007;114(2):97–109.
- Stupp R, et al. Radiotherapy plus concomitant and adjuvant temozolomide for glioblastoma. *N Engl J Med.* 2005;352(10):987–996.
- Wen PY, Kesari S. Malignant gliomas in adults. *N Engl J Med.* 2008;359(5):492–507.
- Singh SK, et al. Identification of a cancer stem cell in human brain tumors. *Cancer Res.* 2003;63(18):5821–5828.
- Singh SK, et al. Identification of human brain tumour initiating cells. *Nature.* 2004;432(7015):396–401.
- Liu G, et al. Analysis of gene expression and chemoresistance of CD133+ cancer stem cells in glioblastoma. *Mol Cancer.* 2006;5:67.
- Cooper LA, et al. The tumor microenvironment strongly impacts master transcriptional regulators and gene expression class of glioblastoma. *Am J Pathol.* 2012;180(5):2108–2119.
- Bailey KM, Wojtkowiak JW, Hashim AI, Gillies RJ. Targeting the metabolic microenvironment of tumors. *Adv Pharmacol.* 2012;65:63–107.
- Lendahl U, Lee KL, Yang H, Poellinger L. Generating specificity and diversity in the transcriptional response to hypoxia. *Nat Rev Genet.* 2009;10(12):821–832.
- Vander Heiden MG, Cantley LC, Thompson CB. Understanding the Warburg effect: the metabolic requirements of cell proliferation. *Science.* 2009;324(5930):1029–1033.
- Gillies RJ, Alger JR, den Hollander JA, Shulman RG. Intracellular pH measured by NMR: methods and results. *Kroc Found Ser.* 1981;15:79–104.
- Gillies RJ, Liu Z, Bhujwala Z. 31P-MRS measurements of extracellular pH of tumors using 3-aminopropylphosphonate. *Am J Physiol.* 1994;267(1 Pt 1):C195–C203.
- Li Z, et al. Hypoxia-inducible factors regulate tumorigenic capacity of glioma stem cells. *Cancer Cell.* 2009;15(6):501–513.
- Rankin EB, Giaccia AJ. The role of hypoxia-inducible factors in tumorigenesis. *Cell Death Differ.* 2008;15(4):678–685.
- Chiche J, Brahimi-Horn MC, Pouyssegur J. Tumour hypoxia induces a metabolic shift causing acidosis: a common feature in cancer. *J Cell Mol Med.* 2010;14(4):771–794.
- Semenza GL. Regulation of mammalian O₂ homeostasis by hypoxia-inducible factor 1. *Annu Rev Cell Dev Biol.* 1999;15:551–578.
- Wykoff CC, Pugh CW, Harris AL, Maxwell PH, Ratcliffe PJ. The HIF pathway: implications for patterns of gene expression in cancer. *Novartis Found Symp.* 2001;240:212–225;discussion 225–231.
- McIntyre A, et al. Carbonic anhydrase IX promotes tumor growth and necrosis in vivo and inhibition enhances anti-VEGF therapy. *Clin Cancer Res.* 2012;18(11):3100–3111.
- Kaluz S, Kaluzová M, Liao SY, Lerman M, Stanbridge EJ. Transcriptional control of the tumor- and hypoxia-marker carbonic anhydrase 9: A one transcription factor (HIF-1) show? *Biochim Biophys Acta.* 2009;1795(2):162–172.
- McDonald PC, Winum JY, Supuran CT, Dedhar S. Recent developments in targeting carbonic anhydrase IX for cancer therapeutics. *Oncotarget.* 2012;3(1):84–97.
- Supuran CT. Carbonic anhydrases: novel therapeutic applications for inhibitors and activators. *Nat Rev Drug Discov.* 2008;7(2):168–181.
- Proescholdt MA, et al. Expression of hypoxia-inducible carbonic anhydrases in brain tumors. *Neuro-oncology.* 2005;7(4):465–475.
- Proescholdt MA, Merrill MJ, Stoerr EM, Lohmeier A, Pohl F, Brawanski A. Function of carbonic anhydrase IX in glioblastoma multiforme. *Neuro-oncology.* 2012;14(11):1357–1366.
- McDonald PC, Dedhar S. Carbonic anhydrase IX (CAIX) as a mediator of hypoxia-induced stress response in cancer cells. *Subcell Biochem.* 2014;75:255–269.
- Gieling RG, Williams KJ. Carbonic anhydrase IX as a target for metastatic disease. *Bioorg Med Chem.* 2013;21(6):1470–1476.
- Ebos JM, Lee CR, Kerbel RS. Tumor and host-mediated pathways of resistance and disease progression in response to antiangiogenic therapy. *Clin Cancer Res.* 2009;15(16):5020–5025.
- Lou Y, et al. Targeting tumor hypoxia: suppression of breast tumor growth and metastasis by novel carbonic anhydrase IX inhibitors. *Cancer Res.* 2011;71(9):3364–3376.

28. Lock FE, et al. Targeting carbonic anhydrase IX depletes breast cancer stem cells within the hypoxic niche. *Oncogene*. 2013;32(44):5210–5219.
29. Supuran CT, Scozzafava A. Carbonic anhydrase inhibitors: aromatic sulfonamides and disulfonamides act as efficient tumor growth inhibitors. *J Enzym Inhib*. 2000;15(6):597–610.
30. Das A, Banik NL, Ray SK. Modulatory effects of acetazolamide and dexamethasone on temozolomide-mediated apoptosis in human glioblastoma T98G and U87MG cells. *Cancer Invest*. 2008;26(4):352–358.
31. Pacchiano F, et al. Ureido-substituted benzenesulfonamides potently inhibit carbonic anhydrase IX and show antimetastatic activity in a model of breast cancer metastasis. *J Med Chem*. 2011;54(6):1896–1902.
32. Bowman RL, Wang Q, Carro A, Verhaak RG, Squatrito M. GlioVis data portal for visualization and analysis of brain tumor expression datasets. *Neuro-oncology*. 2017;19(1):139–141.
33. Brennan CW, et al. The somatic genomic landscape of glioblastoma. *Cell*. 2013;155(2):462–477.
34. Cancer Genome Atlas Research Network. Comprehensive genomic characterization defines human glioblastoma genes and core pathways. *Nature*. 2008;455(7216):1061–1068.
35. Oliva CR, et al. Acquisition of temozolomide chemoresistance in gliomas leads to remodeling of mitochondrial electron transport chain. *J Biol Chem*. 2010;285(51):39759–39767.
36. Marin-Valencia I, et al. Analysis of tumor metabolism reveals mitochondrial glucose oxidation in genetically diverse human glioblastomas in the mouse brain in vivo. *Cell Metab*. 2012;15(6):827–837.
37. Yuen CA, Asuthkar S, Guda MR, Tsung AJ, Velpula KK. Cancer stem cell molecular reprogramming of the Warburg effect in glioblastomas: a new target gleaned from an old concept. *CNS Oncol*. 2016;5(2):101–108.
38. Boroughs LK, DeBerardinis RJ. Metabolic pathways promoting cancer cell survival and growth. *Nat Cell Biol*. 2015;17(4):351–359.
39. Piccirillo SG, et al. Bone morphogenetic proteins inhibit the tumorigenic potential of human brain tumour-initiating cells. *Nature*. 2006;444(7120):761–765.
40. Hottinger AF, Stupp R, Homicsko K. Standards of care and novel approaches in the management of glioblastoma multiforme. *Chin J Cancer*. 2014;33(1):32–39.
41. Stupp R, et al. Effects of radiotherapy with concomitant and adjuvant temozolomide versus radiotherapy alone on survival in glioblastoma in a randomised phase III study: 5-year analysis of the EORTC-NCIC trial. *Lancet Oncol*. 2009;10(5):459–466.
42. Cloughesy TF, et al. Phase I trial of vocimagene amiretrorepvec and 5-fluorocytosine for recurrent high-grade glioma. *Sci Transl Med*. 2016;8(341):341ra75.
43. Stupp R, et al. Maintenance therapy with tumor-treating fields plus temozolomide vs temozolomide alone for glioblastoma: A randomized clinical trial. *JAMA*. 2015;314(23):2535–2543.
44. Oliva CR, Moellering DR, Gillespie GY, Griguer CE. Acquisition of chemoresistance in gliomas is associated with increased mitochondrial coupling and decreased ROS production. *PLoS ONE*. 2011;6(9):e24665.
45. Cong D, et al. Upregulation of NHE1 protein expression enables glioblastoma cells to escape TMZ-mediated toxicity via increased H⁺ extrusion, cell migration and survival. *Carcinogenesis*. 2014;35(9):2014–2024.
46. Hegi ME, et al. MGMT gene silencing and benefit from temozolomide in glioblastoma. *N Engl J Med*. 2005;352(10):997–1003.
47. Marathe K, McVicar N, Li A, Bellyou M, Meakin S, Bartha R. Topiramate induces acute intracellular acidification in glioblastoma. *J Neurooncol*. 2016;130(3):465–472.
48. Lee CY, Lai HY, Chiu A, Chan SH, Hsiao LP, Lee ST. The effects of antiepileptic drugs on the growth of glioblastoma cell lines. *J Neurooncol*. 2016;127(3):445–453.
49. Kaur T, Manchanda S, Saini V, Lakhman SS, Kaur G. Efficacy of anti-epileptic drugs in the treatment of tumor and its associated epilepsy: An in vitro perspective. *Ann Neurosci*. 2016;23(1):33–43.
50. Huppold C, et al. Does valproic acid or levetiracetam improve survival in glioblastoma? A pooled analysis of prospective clinical trials in newly diagnosed glioblastoma. *J Clin Oncol*. 2016;34(7):731–739.
51. McIntyre A, et al. Disrupting hypoxia-induced bicarbonate transport acidifies tumor cells and suppresses tumor growth. *Cancer Res*. 2016;76(13):3744–3755.
52. Swayampakula M, et al. The interactome of metabolic enzyme carbonic anhydrase IX reveals novel roles in tumor cell migration and invadopodia/MMP14-mediated invasion. *Oncogene*. 2017;36(45):6244–6261.
53. Madhavan S, Zenklusen JC, Kotliarov Y, Sahni H, Fine HA, Buetow K. Rembrandt: helping personalized medicine become a reality through integrative translational research. *Mol Cancer Res*. 2009;7(2):157–167.
54. Dunn WB, et al. Procedures for large-scale metabolic profiling of serum and plasma using gas chromatography and liquid chromatography coupled to mass spectrometry. *Nat Protoc*. 2011;6(7):1060–1083.
55. Xia J, Wishart DS. Using MetaboAnalyst 3.0 for comprehensive metabolomics data analysis. *Curr Protoc Bioinformatics*. 2016;55:14.10.1–14.10.91.
56. Kutmon M, et al. PathVisio 3: an extendable pathway analysis toolbox. *PLoS Comput Biol*. 2015;11(2):e1004085.
57. van Iersel MP, et al. Presenting and exploring biological pathways with PathVisio. *BMC Bioinformatics*. 2008;9:399.
58. Kelder T, et al. WikiPathways: building research communities on biological pathways. *Nucleic Acids Res*. 2012;40(Database issue):D1301–D1307.
59. Diers AR, et al. Mitochondrial bioenergetics of metastatic breast cancer cells in response to dynamic changes in oxygen tension: effects of HIF-1 α . *PLoS One*. 2013;8(6):e68348.
60. Hu Y, Smyth GK. ELDA: extreme limiting dilution analysis for comparing depleted and enriched populations in stem cell and other assays. *J Immunol Methods*. 2009;347(1-2):70–78.